AUTOMATED CLOUD OBSERVATION FOR GROUND TELESCOPE OPTIMIZATION

Ben Lane
ExoAnalytic Solutions
Mark W. Jeffries, Jr.
ExoAnalytic Solutions
William Therien
ExoAnalytic Solutions
Hung Nguyen
ExoAnalytic Solutions

ABSTRACT

As the number of man-made objects placed in space each year increases with advancements in commercial, academic and industry, the number of objects required to be detected, tracked, and characterized continues to grow at an exponential rate. Commercial companies, such as ExoAnalytic Solutions, have deployed ground based sensors to maintain track custody of these objects. For the ExoAnalytic Global Telescope Network (EGTN), observation of such objects are collected at the rate of over 10 million unique observations per month (as of September 2017). Currently, the EGTN does not optimally collect data on nights with significant cloud levels. However, a majority of these nights prove to be partially cloudy providing clear portions in the sky for EGTN sensors to observe. It proves useful for a telescope to utilize these clear areas to continue resident space object (RSO) observation. By dynamically updating the tasking with the varying cloud positions, the number of observations could potentially increase dramatically due to increased persistence, cadence, and revisit.

This paper will discuss the recent algorithms being implemented within the EGTN, including the motivation, need, and general design. The use of automated image processing as well as various edge detection methods, including Canny, Sobel, and Marching Squares, on real-time large FOV images of the sky enhance the tasking and scheduling of a ground based telescope is discussed in Section 2. Implementations of these algorithms on single and expanding to multiple telescopes, will be explored. Results of applying these algorithms to the EGTN in real-time and comparison to non-optimized EGTN tasking is presented in Section 3. Finally, in Section 4 we explore future work in applying these throughout the EGTN as well as other optical telescopes.

1. BACKGROUND

As the need for Space Situational Awareness (SSA) exponentially increases at a pace that far exceeds the current Space Surveillance Network (SSN) collection capabilities, commercial SSA is quickly becoming increasingly critical to the space community, including both commercial operators and the warfighter. The EGTN collects an ever-increasing amount of data for GEO and near-GEO objects. Possessing full longitudinal coverage, the EGTN spans the entirety of geostationary equatorial orbit which is the region typically referred to as the GEO belt (Fig. 1). With over 170 telescopes in multiple countries, the network has been operating since 2012 and is currently averaging 400,000 correlated observations per night (as of September 2017). The nightly operation for every sensor in the network is customizable and dynamically allocated, but currently not optimized for localized weather aberrations. At times, remote sites may close prematurely due to declining weather conditions. If the automated remote observatory is open, clouds may still inhibit the collection on specific objects of interest, create non-optimal observing conditions, or a combination of the two. In certain circumstances, sensors become "stuck" (e.g. after slewing to a tasked azimuth and elevation and completing the task, the sensor is unable to determine its current pointing due to a cloud obscuring the frame and preventing image registration) and unable to slew away to continue data collection. This type of situation has led to the design, development, and initial prototyping of the ExoAnalytic Cloud Observer (ECO). ECO is a capability to determine optimal collection strategies based on the available clear space in between clouds as a function

of time. With knowledge of the where the patches are in between clouds and how these patches are changing, individual sensors and eventually entire sites can be optimized to collect in a more intelligent and optimized manner.

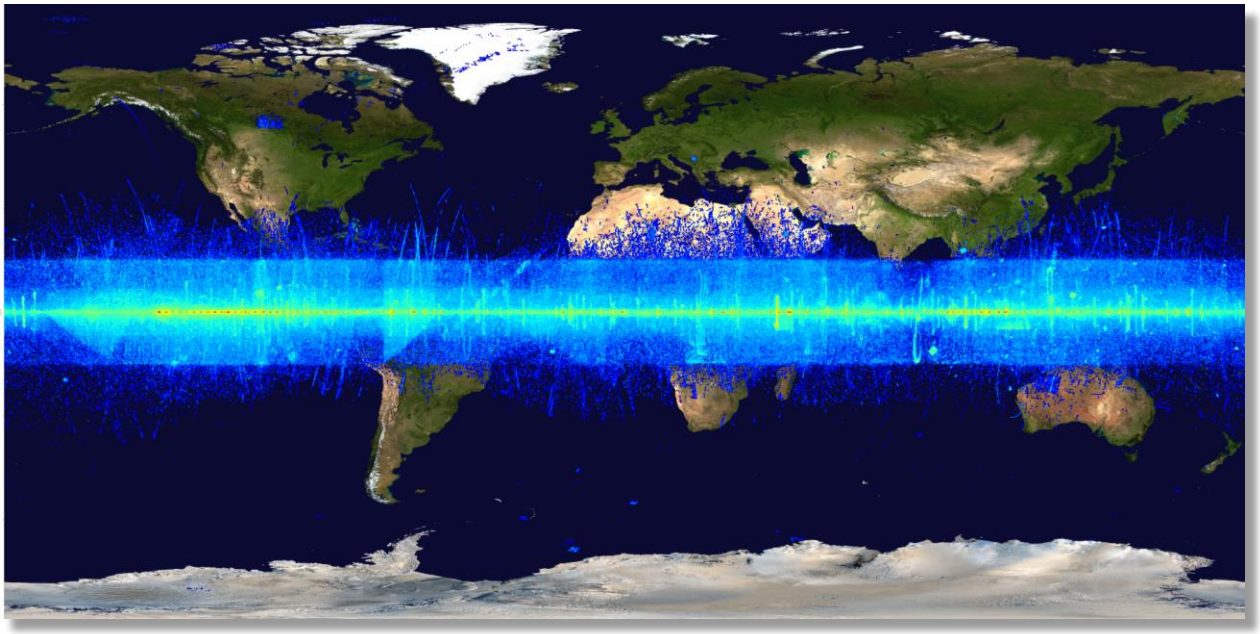

Fig. 1 The EGTN Covering the GEO Belt

2. APPROACH

The approach as applied to the EGTN and the ExoAnalytic Space Operation Center (ESpOC) Sensor is illustrated in Fig. 2. At a given interval, an image of the night sky is captured by the ECO imager. For the results presented in this paper, we used a five minute interval between sky images since this interval balanced the collection of data for each sensor and the amount of cloud movement at our research site. Ideally, the image will capture the entire azimuth and elevation limits available to the specific sensor that is running ECO. ECO then registers the image to determine its pointing. Automated processing is then completed to determine where the location of the clouds are in the ESpOC sensor's coordinate frame. These cloud positions are maintained in ECO for forecasting and historical context that is used in the following iterations.

Next, the ExoAnalytic tasking software, the Basic ESpOC Resource Tasker (BERT), ingests the cloud information to determine tasking for the next object based on the cloud mask received from ECO. The cloud mask essentially is a heatmap of the light and dark spots of the ECO image (Fig. 3). Results of the heatmap are analyzed further in the Section 3. The next tasking is then sent to the ESpOC sensor. Feedback from the ESpOC sensor allows BERT, and subsequently ECO, to confirm optimal tasking using this cloud heatmap. Data is then collected and processed using the updated tasking automatically. Finally, the entire process is repeated at the specified interval. If ECO determines that clouds will obscure the current object at any time, BERT will change the tasking in real time to maintain the optimal collection of the objects of interest.

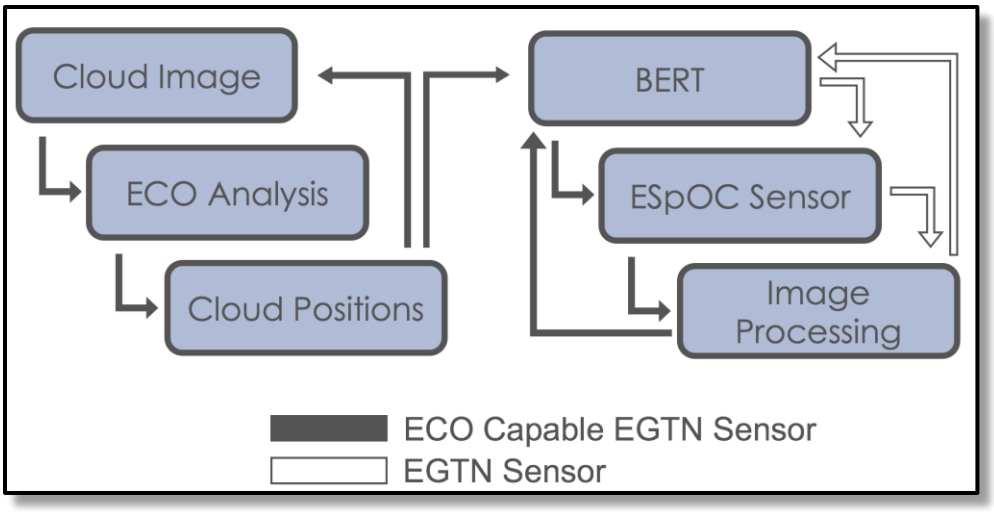

Fig. 2 Automatic Cloud Detection Data Flow

3. INITIAL RESULTS

The first requirement for ECO is to accurately determine the location of clouds. Two approaches have been implemented. The first approach is to determine where the clear patches are, determine where the objects of interest are, and task BERT accordingly. The second approach is to create a heatmap of light areas and allow BERT to determine optimal collection strategy. While the former proved promising, the initial results presented in this paper are from the latter.

Cloud Patch Identification

In order to determine the location of the clear patches, various edge detection techniques were explored. Using the available algorithms in the open source python module Scikit-Image[1], Edge, Sobel, and Marching Squares were applied to a wide variety of sample images collected by the ECO imager over multiple nights. While the Edge and Sobel techniques did provide results that could have been used by ECO, Marching Squares provided the most consistent and accurate edge detection as applied to the sample images collected by the ECO imager. Results of the Marching Squares edge detection as applied to cloud detection is shown in Fig. 3.

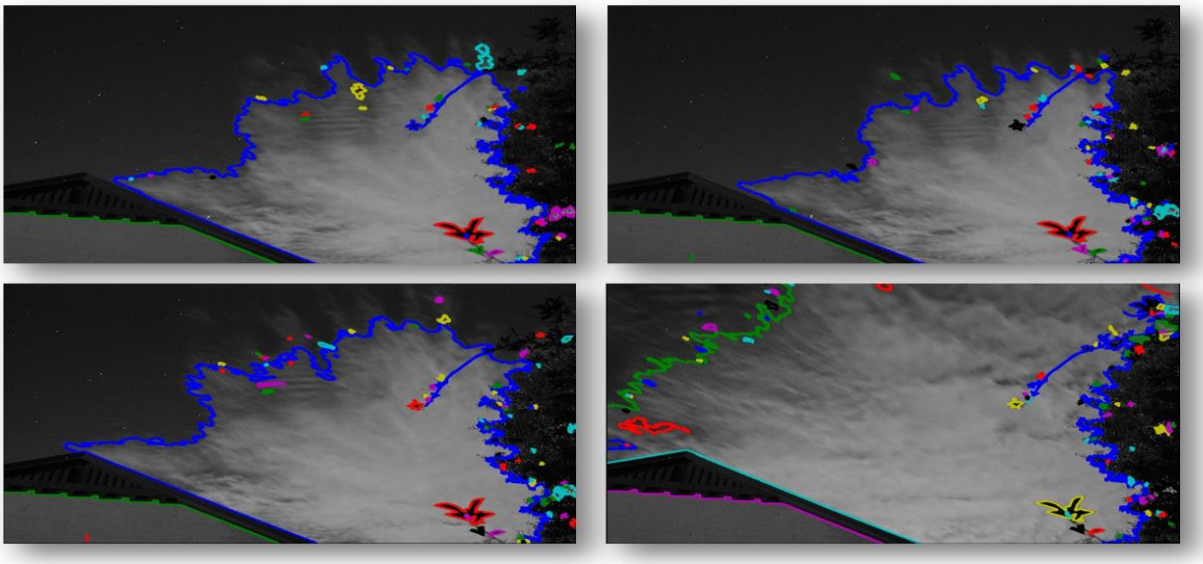

Fig. 3 Edge Detection of Clouds Using Marching Squares Technique

Next, the cloud patches are mapped into the reference frame of the ESpOC sensor; in this case, azimuth and elevation. The RSOs of interest are also mapped into the same ESpOC sensor reference frame. With the cloud patches and RSOs in the same reference frame, ECO determines which RSOs are obscured by the clouds and therefore not to be tasked by BERT. An example of determining what objects are obscured by clouds and thus unavailable for tasking is shown in Fig. 4. The cyan outline is the edge of the clouds as detected by ECO. The dots and corresponding five-digit number is the RSO location mapped onto the ECO image and the RSOs NORAD ID. If the dot is green, the object is available for tasking as it is not obscured by clouds. If it is red, ECO has determined that the object is obscured and is unavailable for tasking. Note that the patches determined by ECO are in fact the clouds and not the clear sky that the ESpOC sensor will use.

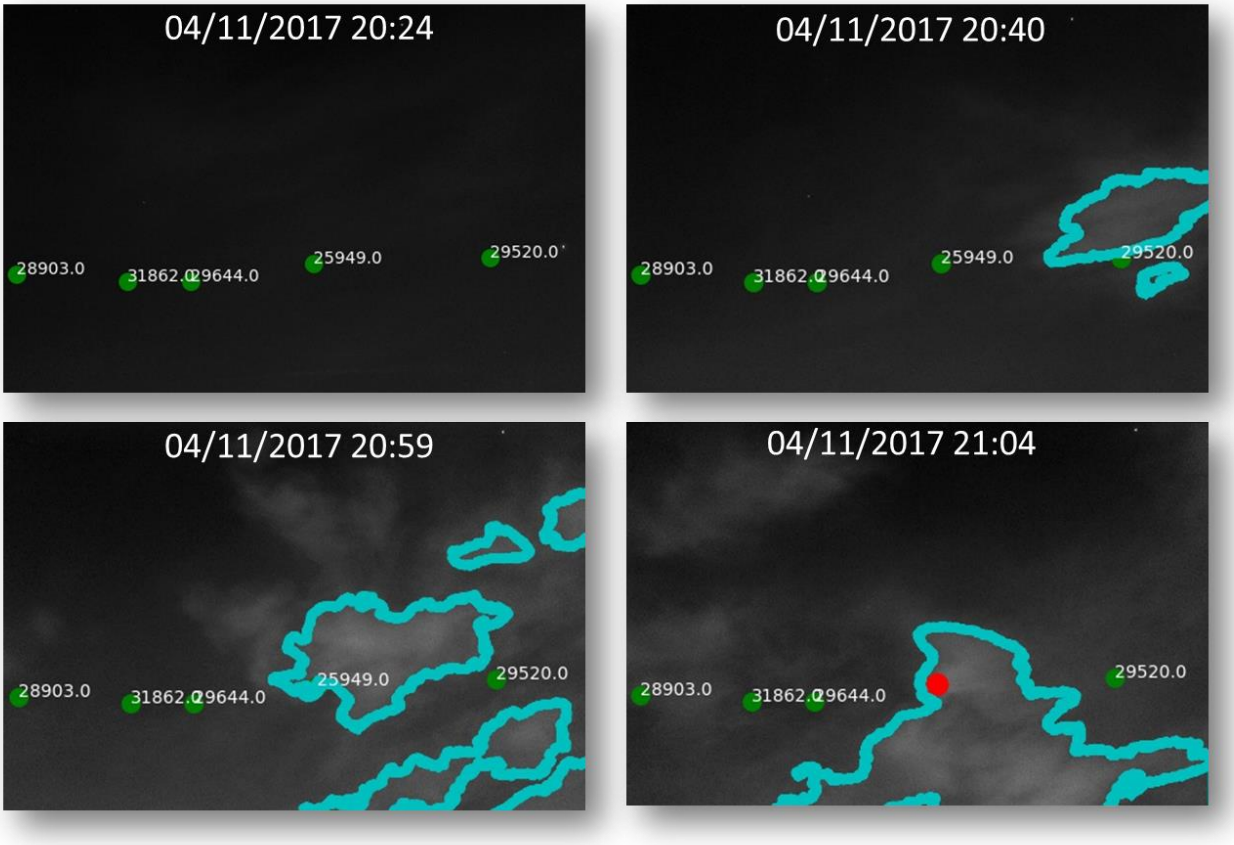

Fig. 4 Available Objects for BERT Tasking Based on Cloud Patch Identification

Cloud Masking

While cloud patch identification proved useful in certain circumstances, it proved difficult to implement a tasking schedule without relying on additional optimization techniques that would utilize the output of ECO. Because of this, we explored a way to inform our existing tasking software of possible cloud obscuration, allowing it to determine tasking while minimizing the need for external algorithms.

The results of the cloud masking is shown in Fig. 5. Similar to our approach for cloud patch identification, an image is collected by ECO (Fig. 5, left) and the pixels are individually mapped into the ESpOC sensor reference frame. After

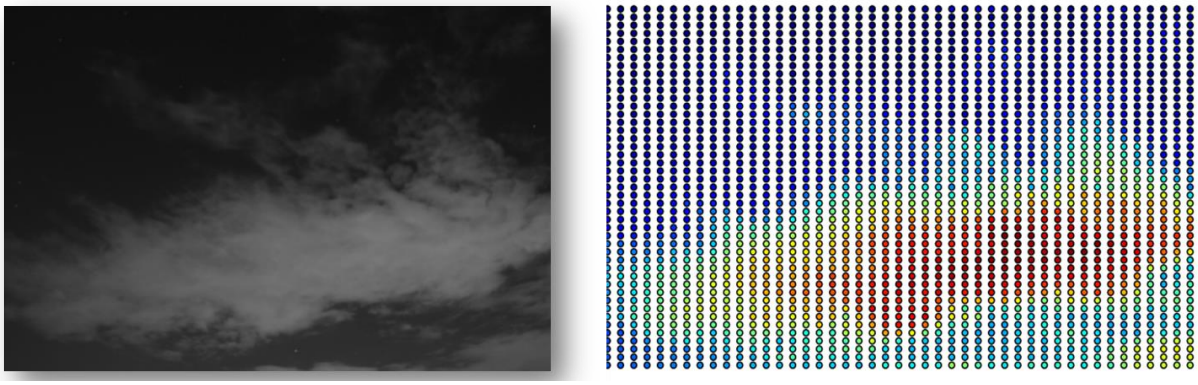

Fig. 5: ECO Image (Left) and Cloud Mask Heatmap

normalizing the brightness values of the individual pixels, the image is binned and quantized. The bin sizes are dependent on the size of the image, bandwidth of ECO, and desired accuracy of the heatmap. The azimuth and elevation values of these bins are also calculated. Next, the binned values are mapped into light and dark areas (Fig. 5, right), with red being more light and blue being more dark, relative to the overall brightness of the image. Finally, the azimuth, elevation, and brightness value is sent to BERT, where tasking is determined based on current and future tasking requirements.

Collection Results

To test the cloud detection results of ECO we designed an experiment utilizing two identical, co-located telescopes at the ExoAnalytic Research and Design Center (RDC) in Colorado Springs, CO, USA. Completing the experiment with two sensors in this manner allows for simultaneous collections with one sensor utilizing ECO and the other to perform nominal operations. Furthermore, observing conditions are constantly changing (due to weather, cloud cover, moon position, etc.) eliminating the possibility of comparing different nights using the same sensor for this type of analysis as weather is never identical one night to the next.

Table 1: Tasked GEO Satellites

NORAD ID	Name	Longitude (°E)
24812	GALAXY-25	-93.065
26402	ECHOSTAR-6	-96.17
28903	SPACEWAY-2	-99.058
29494	DIRECTV-9S	-101.055
37218	SKYTERRA-1	-101.261
37748	SES-3	-102.969
35491	GOES-14	-104.495
29644	AMC-18	-104.91
26624	ANIK-F1	-107.268
25949	TELSTAR-12	-109.164
27426	DIRECTV-5	-110.09
35496	TERRESTAR-1	-111.023
29643	WILDBLUE-1	-111.153
29162	SATEMEX-6	-112.985
37843	VIASAT-1	-115.08

39360	SIRIUS-FM-6	-116.131
39122	SATMEX-8	-116.793
31102	ANIK-F3	-118.707
27854	GALAXY-23	-120.974

The developed experiment consisted of selecting a subset of GEO-stationary and GEO-inclined satellites that were within the field-of-regard (FOR) of both sensors. The subset of objects was extracted from the space-track.org catalog and is included as Table 1. Due to the confines of the observatory enclosure, the FOR overlap between both sensors limited RSO selection to approximately 30^{o} of the GEO belt. Taking weather variability into account, we present results from two consecutive nights of observations, 2017 August 29 and 2017 August 30. August 29 was mostly clear for the entire night and we treat this as the baseline metric for our study. August 30 was partly cloudy and is used to display the improvement ECO adds to observing results. In all cases, both sensors were tasked to track the RSOs included in Table 1 following a greedy salesman tasking pattern with a dwell time of 5 minutes per object.

On both nights of collection the same two sensors were utilized, RDC-1148 and RDC-1229. On August 29, both sensors collected without ECO in order to generate a data set to compare the collection results sensor-to-sensor over the course of a single night. We refer to this collection model as the baseline. For the second data set on August 30, RDC-1148 utilized the results of ECO while RDC-1229 had no change in operations from the baseline collection method. Results from this baseline collection are seen in the left side panel of Fig. 7, with the ECO results located on the right side panel. Numeric results are tabulated in Table 2.

The baseline results illustrate that both sensors exhibited similar performance. On some targets, RDC-1148 possessed more correlated observations on a particular target while RDC-1229 collected more on others. This type of behavior is anticipated over the course of an observing night as the numbers will not be identical due to varying observing conditions as well as the presence of other artifacts on the image (e.g., hot pixels, RSO overlap with a star, closely spaced objects). Fig. 8 displays the difference between the two sensors by determining the variance in the number of correlated observations. We subtract the number of correlated observations of RDC-1148 by the number of correlated observations of RDC-1229. In this definition, positive numbers indicate that RDC-1148 had an increased number of correlated detections on that particular target. These results are seen as the blue histogram bars of the left side panel of Fig. 8. For the baseline collection we anticipate the difference in number of correlated detections to be

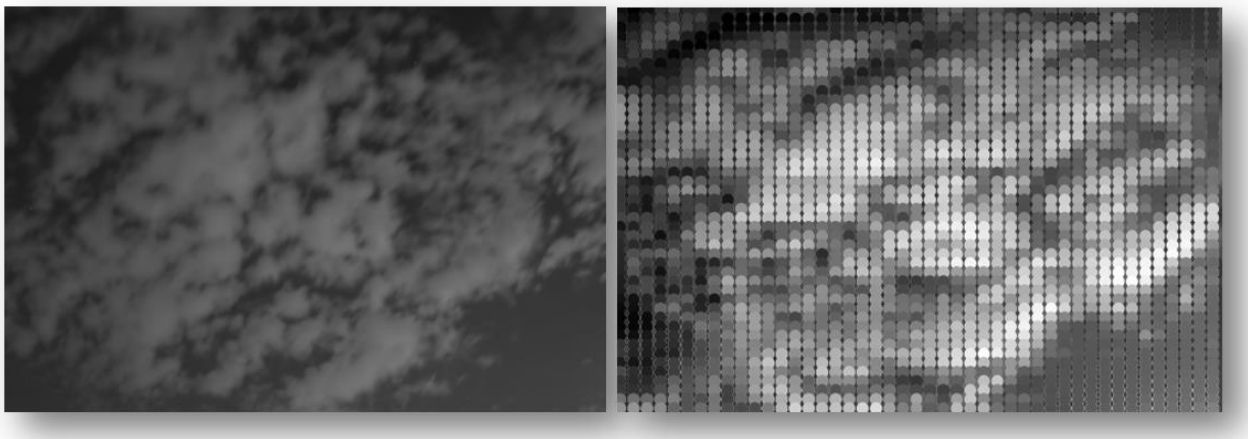

Fig. 6 ECO Image and Cloud Masking for August 30

approximately symmetric about zero. This behavior is seen in the data as the difference between number of correlated observations in the control collect is less than 70 in all cases and averages to +4.

With ECO employed on RDC-1148, it is clear to see the improvement in number of correlated observations for sky positions that were detected to be free from cloud by ECO. This is seen by comparing the grey histogram bars of RDC-1148 to the blue histogram bars of RDC-1229 in the right side panel of Fig. 7. RSOs further to the west (< 102 ^{o}E) show little to no observations on RDC-1148 while RDC-1229 still shows correlated detections on these objects.

As RDC-1229 was completing the nominal tasking without ECO, it would have slewed to all objects in the task list regardless of cloud position. If a thin layer of cloud is present in a portion of the sky, it is possible for RDC-1229 to collect on the target while ECO would have instructed RDC-1148 to avoid that area of the sky. When observing through a cloud, both photometric and astrometric uncertainty will increase causing orbit determination and other analysis to become less accurate. The authors save the study of data degradation as a result of observing through clouds as the study of a future paper.

The grey histogram bars on the left side panel of Fig. 8 further illustrate the improvement seen when utilizing ECO. Positive values on this panel indicate that more correlated observations were present on RDC-1148 compared to RDC-1229 for the RSO in question. If ECO is believed to positively affecting the observing results, the trend of this delta should be soundly positive which is seen in the figure as well as the average value of +22.

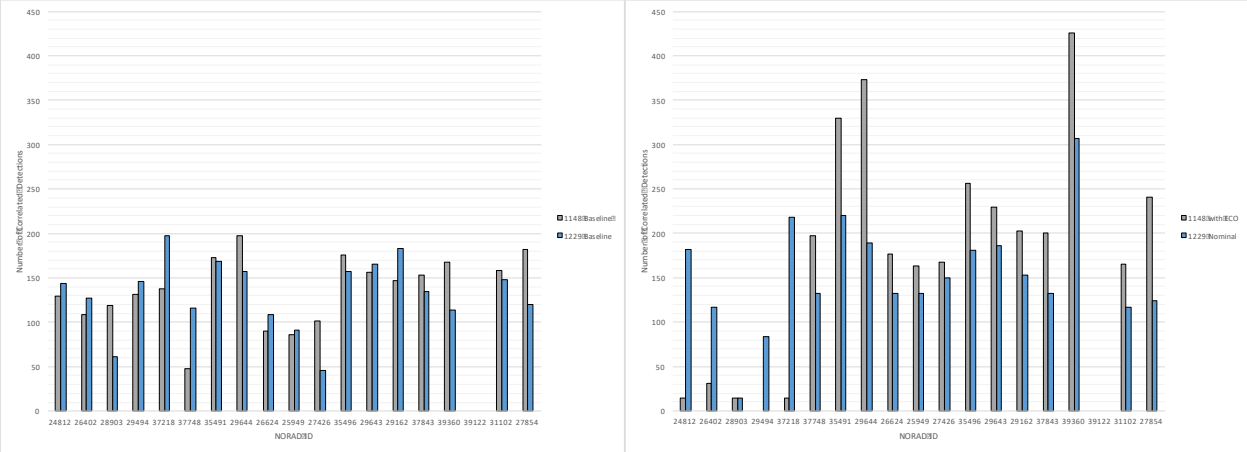

Fig. 7: Nightly Sensor Comparison. Control collect is displayed on the left hand panel and results with ECO employed on sensor 1148 seen on the right hand side.

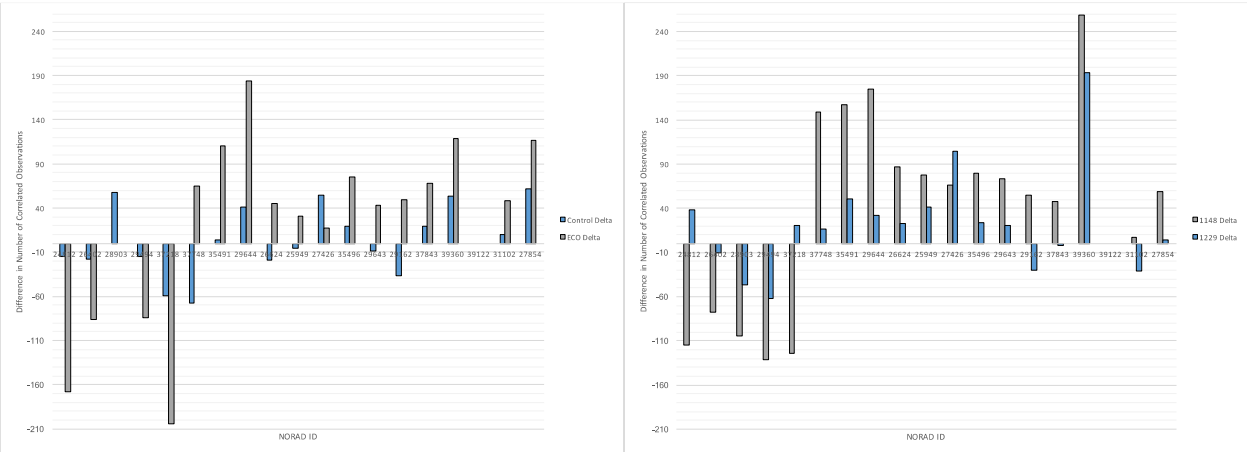

Fig. 8: Difference in number of correlated detections on given collection runs. Right hand panel compares sensors night-to-night. Left hand panel compares single night results. Difference is taken to be Sensor 1148 minus Sensor 1229 in all cases.

Table 2: Results where values are number of correlated detections

	2017-08-29		2017-08-30					
NORAD ID	1148	1229	1148	1229	Control Delta	ECO Delta	1148 Delta	1229 Delta
24812	129	144	14	182	-15	-168	-115	38
26402	109	127	31	117	-18	-86	-78	-10
28903	119	61	14	14	58	0	-105	-47
29494	131	146	0	84	-15	-84	-131	-62
37218	138	197	14	218	-59	-204	-124	21
37748	48	116	197	132	-68	65	149	16
35491	173	169	330	220	4	110	157	51
29644	198	157	373	189	41	184	175	32
26624	90	109	177	132	-19	45	87	23
25949	86	91	163	132	-5	31	77	41
27426	101	46	167	150	55	17	66	104
35496	176	157	256	181	19	75	80	24
29643	156	165	229	186	-9	43	73	21
29162	147	183	202	153	-36	49	55	-30
37843	153	134	200	132	19	68	47	-2
39360	168	114	426	307	54	119	258	193
39122	0	0	0	0	0	0	0	0
31102	158	148	165	117	10	48	7	-31
27854	182	120	241	124	62	117	59	4

4. FUTURE WORK

While the Marching Squares algorithm was selected for implementation in ECO for edge detection in the prototype, additional research, testing, and evaluation of other algorithms, including Sobel and Edge, is necessary before final determination. Further, multiple edge detection algorithms may be implemented and ran in parallel to provide an aggregate solution that improves cloud patch determination.

Additional research into how to optimize a collection schedule using the cloud patch identification technique is required before implementing the approach in ECO. Various optimization strategies will need to be leveraged to determine what objects are tasked in what order to obtain maximum collection time, given a series of constraints that may be dynamically updated as time progresses. For example, one strategy may be weighting an object based on revisit rate, number or observations, priority, and collection duration. This strategy may be updated dynamically as ECO determines cloud motion, requiring BERT to reprioritize. Further, these optimization techniques may be used in conjunction with the cloud mask heatmap to determine likelihood of successful collects, given current and future positions of clouds.

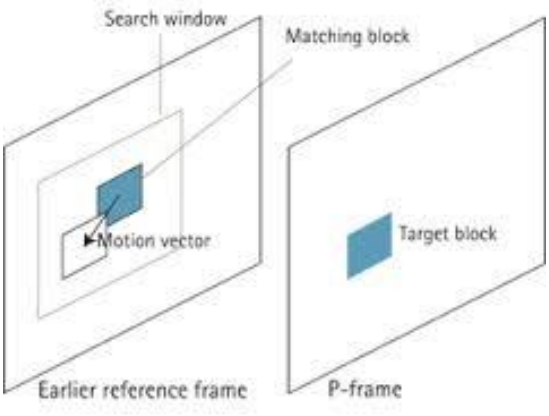

Fig. 9 Motion Vector Analysis

As clouds often do not maintain their exact shape and continually change, models should adapt to their changing nature. Further cloud modeling and motion analysis will be investigated to better predict cloud deformation and evolution. Applying motion vector analysis (MVA) to such a model, can provide the ability to determine changes that occur frame-to-frame. MVA is the method of follow to motion of a block of pixels frame-to-frame (Fig. 9). Matching the pixel blocks on subsequent frames provides a scenario in which cloud patterns may be tracked as the progress across the image.

Additionally, MVA can assist in the identification of multilayered cloud movement in order to predict the overall movement of clouds. With cloud patches positively identified and their motion correctly predicted, this information will be incorporated into ECO and passed along to BERT for tasking considerations. Research in this area has shown that the application of MVA to areas of image processing can provide promising results. [2]

Fig. 10 below depicts our proposed approach of using MVA for cloud forecasting. ECO collects a reference frame of the night sky for use in cloud patch identification and/or cloud masking. Subsequent frames from ECO are used to create the velocity vectors of the clouds. Next the velocity vectors are used to predict the coarse motion of the clouds at the next time of collect. The forecast is also tested against truth for validation of the forecast model and used in subsequent updates to the forecast. Finally, the forecasted new positions of the clouds are used to refine the task optimization portion of ECO for further refinement.

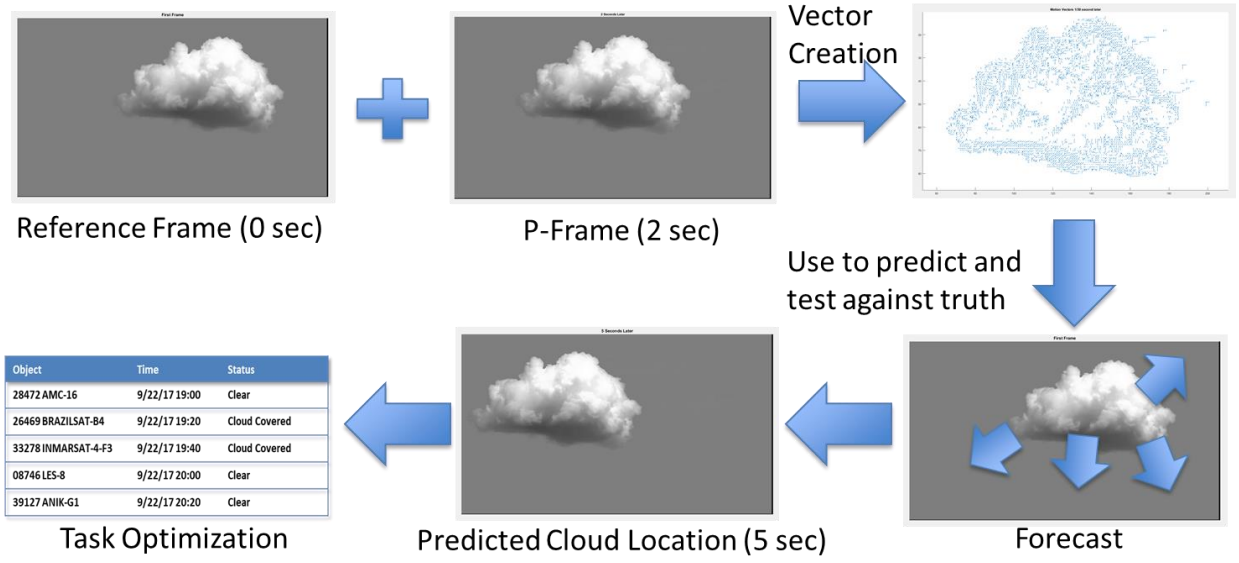

Fig. 10 Motion Vector Analysis Applied to Cloud Forecasting

5. SUMMARY

The desire and need for relevant, timely, persistent SSA at GEO has grown at an exponential rate. The EGTN, a growing global network of ground-based EO sensors, has continued to provide constant SSA at GEO for the past five years. As the EGTN continues to grow and evolve, additional technologies and techniques to optimize collection at the individual sensor and at the site will further increase the value of the EGTN.

In this paper we discussed the need for increased data collection and the initial approach for ECO. Results were shown for cloud patch identification as well as a cloud mask heatmap. An observing campaign utilizing two identical sensors, one running ECO and one running the current nominal tasking software, as well as the two sensors running the nominal tasking software as a baseline metric was employed as a real-time test of the ECO approach. The promising initial results show that ECO improves not only the number of observations on a given object, but also optimized collection on an object that would have been missed due to cloud obscuration.

Finally, we discussed the potential application of ECO on forecasting the movement of clouds and subsequent availability of objects in cloud patches as a function of time. This could further enhance sensor tasking and could potentially be used in adjacent mission areas that rely on accurate knowledge of time dependent spatial object motion.

6. REFERENCES

[1] Scikit-Image. Retrieved September 7, 2016, from http://scikit-image.org/

[2] Nguyen, Hung Viet; *Image processing and analysis of cardiomyocyte contractility and quantification of Western Blots*, San Diego State University, 2013-06-10